Measurements of Normalized Differential Cross Sections of Inclusive π^0 and K_S^0 Production in e^+e^- Annihilation at Energies from 2.2324 to 3.6710 GeV

M. Ablikim,[1] M. N. Achasov,[12,b] P. Adlarson,[72] M. Albrecht,[4] R. Aliberti,[33] A. Amoroso,[71a,71c] M. R. An,[37] Q. An,[68,55] Y. Bai,[54] O. Bakina,[34] R. Baldini Ferroli,[27a] I. Balossino,[28a] Y. Ban,[44,g] V. Batozskaya,[1,42] D. Becker,[33] K. Begzsuren,[30] N. Berger,[33] M. Bertani,[27a] D. Bettoni,[28a] F. Bianchi,[71a,71c] E. Bianco,[71a,71c] J. Bloms,[65] A. Bortone,[71a,71c] I. Boyko,[34] R. A. Briere,[5] A. Brueggemann,[65] H. Cai,[73] X. Cai,[1,55] A. Calcaterra,[27a] G. F. Cao,[1,60] N. Cao,[1,60] S. A. Cetin,[59a] J. F. Chang,[1,55] W. L. Chang,[1,60] G. R. Che,[41] G. Chelkov,[34,a] C. Chen,[41] Chao Chen,[52] G. Chen,[1] H. S. Chen,[1,60] M. L. Chen,[1,55] S. J. Chen,[40] S. M. Chen,[58] T. Chen,[1,60] X. R. Chen,[29,60] X. T. Chen,[1,60] Y. B. Chen,[1,55] Z. J. Chen,[24,h] W. S. Cheng,[71c] S. K. Choi,[52] X. Chu,[41] G. Cibinetto,[28a] F. Cossio,[71c] J. J. Cui,[47] H. L. Dai,[1,55] J. P. Dai,[76] A. Dbeyssi,[18] R. E. de Boer,[4] D. Dedovich,[34] Z. Y. Deng,[1] A. Denig,[33] I. Denysenko,[34] M. Destefanis,[71a,71c] F. De Mori,[71a,71c] Y. Ding,[38] Y. Ding,[32] J. Dong,[1,55] L. Y. Dong,[1,60] M. Y. Dong,[1,55,60] X. Dong,[73] S. X. Du,[78] Z. H. Duan,[40] P. Egorov,[34,a] Y. L. Fan,[73] J. Fang,[1,55] S. S. Fang,[1,60] W. X. Fang,[1] Y. Fang,[1] R. Farinelli,[28a] L. Fava,[71b,71c] F. Feldbauer,[4] G. Felici,[27a] C. Q. Feng,[68,55] J. H. Feng,[56] K. Fischer,[66] M. Fritsch,[4] C. Fritzsch,[65] C. D. Fu,[1] H. Gao,[60] X. L. Gao,[68,m] Y. N. Gao,[44,g] Yang Gao,[68,55] S. Garbolino,[71c] I. Garzia,[28a,28b] P. T. Ge,[73] Z. W. Ge,[40] C. Geng,[56] E. M. Gersabeck,[64] A. Gilman,[66] K. Goetzen,[13] L. Gong,[38] W. X. Gong,[1,55] W. Gradl,[33] M. Greco,[71a,71c] L. M. Gu,[40] M. H. Gu,[1,55] Y. T. Gu,[15] C. Y. Guan,[1,60] A. Q. Guo,[29,60] L. B. Guo,[39] R. P. Guo,[46] Y. P. Guo,[11,f] A. Guskov,[34,a] W. Y. Han,[37] X. Q. Hao,[19] F. A. Harris,[62] K. K. He,[52] K. L. He,[1,60] F. H. Heinsius,[4] C. H. Heinz,[33] Y. K. Heng,[1,55,60] C. Herold,[57] G. Y. Hou,[1,60] Y. R. Hou,[60] Z. L. Hou,[1] H. M. Hu,[1,60] J. F. Hu,[53,i] T. Hu,[1,55,60] Y. Hu,[1] G. S. Huang,[68,55] K. X. Huang,[56] L. Q. Huang,[29,60] X. T. Huang,[47] Y. P. Huang,[1] Z. Huang,[44,g] T. Hussain,[70] N. Hüsken,[26,33] W. Imoehl,[26] M. Irshad,[68,55] J. Jackson,[26] S. Jaeger,[4] S. Janchiv,[30] E. Jang,[52] J. H. Jeong,[52] Q. Ji,[1] Q. P. Ji,[19] X. B. Ji,[1,60] X. L. Ji,[1,55] Y. Y. Ji,[47] Z. K. Jia,[68,55] P. C. Jiang,[44,g] S. S. Jiang,[37] X. S. Jiang,[1,55,60] Y. Jiang,[60] J. B. Jiao,[47] Z. Jiao,[22] S. Jin,[40] Y. Jin,[63] M. Q. Jing,[1,60] T. Johansson,[72] S. Kabana,[31] N. Kalantar-Nayestanaki,[61] X. L. Kang,[9] X. S. Kang,[38] R. Kappert,[61] M. Kavatsyuk,[61] B. C. Ke,[78] I. K. Keshk,[4] A. Khoukaz,[65] R. Kiuchi,[1] R. Kliemt,[13] L. Koch,[35] O. B. Kolcu,[59a] B. Kopf,[4] M. Kuemmel,[4] M. Kuessner,[4] A. Kupsc,[42,72] W. Kühn,[35] J. J. Lane,[64] J. S. Lange,[35] P. Larin,[18] A. Lavania,[25] L. Lavezzi,[71a,71c] T. T. Lei,[68,k] Z. H. Lei,[68,55] H. Leithoff,[33] M. Lellmann,[33] T. Lenz,[33] C. Li,[41] C. Li,[45] C. H. Li,[37] Cheng Li,[68,55] D. M. Li,[78] F. Li,[1,55] G. Li,[1] H. Li,[49] H. Li,[68,55] H. B. Li,[1,60] H. J. Li,[19] H. N. Li,[53,i] J. Q. Li,[4] J. S. Li,[56] J. W. Li,[47] Ke Li,[1] L. J. Li,[1,60] L. K. Li,[1] Lei Li,[3] M. H. Li,[41] P. R. Li,[36,j,k] S. X. Li,[11] S. Y. Li,[58] T. Li,[47] W. D. Li,[1,60] W. G. Li,[1] X. H. Li,[68,55] X. L. Li,[47] Xiaoyu Li,[1,60] Y. G. Li,[44,g] Z. X. Li,[15] Z. Y. Li,[56] C. Liang,[40] H. Liang,[32] H. Liang,[1,60] H. Liang,[68,55] Y. F. Liang,[51] Y. T. Liang,[29,60] G. R. Liao,[14] L. Z. Liao,[47] J. Libby,[25] A. Limphirat,[57] C. X. Lin,[56] D. X. Lin,[29,60] T. Lin,[1] B. J. Liu,[1] C. Liu,[32] C. X. Liu,[1] D. Liu,[18,68] F. H. Liu,[50] Fang Liu,[1] Feng Liu,[6] G. M. Liu,[53,i] H. Liu,[36,j,k] H. B. Liu,[15] H. M. Liu,[1,60] Huanhuan Liu,[1] Huihui Liu,[20] J. B. Liu,[68,55] J. L. Liu,[69] J. Y. Liu,[1,60] K. Liu,[1] K. Y. Liu,[38] Ke Liu,[21] L. Liu,[68,55] Lu Liu,[41] M. H. Liu,[11,f] P. L. Liu,[1] Q. Liu,[60] S. B. Liu,[68,55] T. Liu,[11,f] W. K. Liu,[41] W. M. Liu,[68,55] X. Liu,[36,j,k] Y. Liu,[36,j,k] Y. B. Liu,[41] Z. A. Liu,[1,55,60] Z. Q. Liu,[47] X. C. Lou,[1,55,60] F. X. Lu,[56] H. J. Lu,[22] J. G. Lu,[1,55] X. L. Lu,[1] Y. Lu,[7] Y. P. Lu,[1,55] Z. H. Lu,[1,60] C. L. Luo,[39] M. X. Luo,[77] T. Luo,[11,f] X. L. Luo,[1,55] X. R. Lyu,[60] Y. F. Lyu,[41] F. C. Ma,[38] H. L. Ma,[1] L. L. Ma,[47] M. M. Ma,[1,60] Q. M. Ma,[1] R. Q. Ma,[1,60] R. T. Ma,[60] X. Y. Ma,[1,55] Y. Ma,[44,g] F. E. Maas,[18] M. Maggiora,[71a,71c] S. Maldaner,[4] S. Malde,[66] Q. A. Malik,[70] A. Mangoni,[27b] Y. J. Mao,[44,g] Z. P. Mao,[1] S. Marcello,[71a,71c] Z. X. Meng,[63] J. G. Messchendorp,[13,61] G. Mezzadri,[28a] H. Miao,[1,60] T. J. Min,[40] R. E. Mitchell,[26] X. H. Mo,[1,55,60] N. Yu. Muchnoi,[12,b] Y. Nefedov,[34] F. Nerling,[18,d] I. B. Nikolaev,[12,b] Z. Ning,[1,55] S. Nisar,[10,l] Y. Niu,[47] S. L. Olsen,[60] Q. Ouyang,[1,55,60] S. Pacetti,[27b,27c] X. Pan,[11,f] Y. Pan,[54] A. Pathak,[32] Y. P. Pei,[68,55] M. Pelizaeus,[4] H. P. Peng,[68,55] K. Peters,[13,d] J. L. Ping,[39] R. G. Ping,[1,60] S. Plura,[33] S. Pogodin,[34] V. Prasad,[68,55] F. Z. Qi,[1] H. Qi,[68,55] H. R. Qi,[58] M. Qi,[40] T. Y. Qi,[11,f] S. Qian,[1,55] W. B. Qian,[60] Z. Qian,[56] C. F. Qiao,[60] J. J. Qin,[69] L. Q. Qin,[14] X. P. Qin,[11,f] X. S. Qin,[47] Z. H. Qin,[1,55] J. F. Qiu,[1] S. Q. Qu,[58] K. H. Rashid,[70] C. F. Redmer,[33] K. J. Ren,[37] A. Rivetti,[71c] V. Rodin,[61] M. Rolo,[71c] G. Rong,[1,60] Ch. Rosner,[18] S. N. Ruan,[41] A. Sarantsev,[34,c] Y. Schelhaas,[33] C. Schnier,[4] K. Schoenning,[72] M. Scodeggio,[28a,28b] K. Y. Shan,[11,f] W. Shan,[23] X. Y. Shan,[68,55] J. F. Shangguan,[52] L. G. Shao,[1,60] M. Shao,[68,55] C. P. Shen,[11,f] H. F. Shen,[1,60] W. H. Shen,[60] X. Y. Shen,[1,60] B. A. Shi,[60] H. C. Shi,[68,55] J. Y. Shi,[1] Q. Q. Shi,[52] R. S. Shi,[1,60] X. Shi,[1,55] J. J. Song,[19] W. M. Song,[32,1] Y. X. Song,[44,g] S. Sosio,[71a,71c] S. Spataro,[71a,71c] F. Stieler,[33] P. P. Su,[52] Y. J. Su,[60] G. X. Sun,[1] H. Sun,[60] H. K. Sun,[1] J. F. Sun,[19] L. Sun,[73] S. S. Sun,[1,60] T. Sun,[1,60] W. Y. Sun,[32] Y. J. Sun,[68,55] Y. Z. Sun,[1] Z. T. Sun,[47] Y. H. Tan,[73] Y. X. Tan,[68,55] C. J. Tang,[51] G. Y. Tang,[1] J. Tang,[56] L. Y. Tao,[69] Q. T. Tao,[24,h] M. Tat,[66] J. X. Teng,[68,55] V. Thoren,[72] W. H. Tian,[49] Y. Tian,[29,60] I. Uman,[59b] B. Wang,[68,55] B. Wang,[1] B. L. Wang,[60] C. W. Wang,[40] D. Y. Wang,[44,g] F. Wang,[69] H. J. Wang,[36,j,k] H. P. Wang,[1,60]

K. Wang,[1,55] L. L. Wang,[1] M. Wang,[47] M. Z. Wang,[44,g] Meng Wang,[1,60] S. Wang,[11,f] S. Wang,[14] T. Wang,[11,f] T. J. Wang,[41] W. Wang,[56] W. H. Wang,[73] W. P. Wang,[68,55] X. Wang,[44,g] X. F. Wang,[36,j,k] X. L. Wang,[11,f] Y. Wang,[58] Y. D. Wang,[43] Y. F. Wang,[1,55,60] Y. H. Wang,[45] Y. Q. Wang,[1] Yaqian Wang,[17,1] Z. Wang,[1,55] Z. Y. Wang,[1,60] Ziyi Wang,[60] D. H. Wei,[14] F. Weidner,[65] S. P. Wen,[1] D. J. White,[64] U. Wiedner,[4] G. Wilkinson,[66] M. Wolke,[72] L. Wollenberg,[4] J. F. Wu,[1,60] L. H. Wu,[1] L. J. Wu,[1,60] X. Wu,[11,f] X. H. Wu,[32] Y. Wu,[68] Y. J. Wu,[29] Z. Wu,[1,55] L. Xia,[68,55] T. Xiang,[44,g] D. Xiao,[36,j,k] G. Y. Xiao,[40] H. Xiao,[11,f] S. Y. Xiao,[1] Y. L. Xiao,[11,f] Z. J. Xiao,[39] C. Xie,[40] X. H. Xie,[44,g] Y. Xie,[47] Y. G. Xie,[1,55] Y. H. Xie,[6] Z. P. Xie,[68,55] T. Y. Xing,[1,60] C. F. Xu,[1,60] C. J. Xu,[56] G. F. Xu,[1] H. Y. Xu,[63] Q. J. Xu,[16] X. P. Xu,[52] Y. C. Xu,[75] Z. P. Xu,[40] F. Yan,[11,f] L. Yan,[11,f] W. B. Yan,[68,55] W. C. Yan,[78] H. J. Yang,[48,e] H. L. Yang,[32] H. X. Yang,[1] Tao Yang,[1] Y. F. Yang,[41] Y. X. Yang,[1,60] Yifan Yang,[1,60] M. Ye,[1,55] M. H. Ye,[8] J. H. Yin,[1] Z. Y. You,[56] B. X. Yu,[1,55,60] C. X. Yu,[41] G. Yu,[1,60] T. Yu,[69] X. D. Yu,[44,g] C. Z. Yuan,[1,60] L. Yuan,[2] S. C. Yuan,[1] X. Q. Yuan,[1] Y. Yuan,[1,60] Z. Y. Yuan,[56] C. X. Yue,[37] A. A. Zafar,[70] F. R. Zeng,[47] X. Zeng,[6] Y. Zeng,[24,h] X. Y. Zhai,[32] Y. H. Zhan,[56] A. Q. Zhang,[1,60] B. L. Zhang,[1,60] B. X. Zhang,[1] D. H. Zhang,[41] G. Y. Zhang,[19] H. Zhang,[68] H. H. Zhang,[56] H. H. Zhang,[32] H. Q. Zhang,[1,55,60] H. Y. Zhang,[1,55] J. L. Zhang,[74] J. Q. Zhang,[39] J. W. Zhang,[1,55,60] J. X. Zhang,[36,j,k] J. Y. Zhang,[1] J. Z. Zhang,[1,60] Jianyu Zhang,[1,60] Jiawei Zhang,[1,60] L. M. Zhang,[58] L. Q. Zhang,[56] Lei Zhang,[40] P. Zhang,[1] Q. Y. Zhang,[37,78] Shuihan Zhang,[1,60] Shulei Zhang,[24,h] X. D. Zhang,[43] X. M. Zhang,[1] X. Y. Zhang,[47] X. Y. Zhang,[52] Y. Zhang,[66] Y. T. Zhang,[78] Y. H. Zhang,[1,55] Yan Zhang,[68,55] Yao Zhang,[1] Z. H. Zhang,[1] Z. L. Zhang,[32] Z. Y. Zhang,[41] Z. Y. Zhang,[73] G. Zhao,[1] J. Zhao,[37] J. Y. Zhao,[1,60] J. Z. Zhao,[1,55] Lei Zhao,[68,55] Ling Zhao,[1] M. G. Zhao,[41] S. J. Zhao,[78] Y. B. Zhao,[1,55] Y. X. Zhao,[29,60] Z. G. Zhao,[68,55] A. Zhemchugov,[34,a] B. Zheng,[69] J. P. Zheng,[1,55] Y. H. Zheng,[60] B. Zhong,[39] C. Zhong,[69] X. Zhong,[56] H. Zhou,[47] L. P. Zhou,[1,60] X. Zhou,[73] X. K. Zhou,[60] X. R. Zhou,[68,55] X. Y. Zhou,[37] Y. Z. Zhou,[11,f] J. Zhu,[41] K. Zhu,[1] K. J. Zhu,[1,55,60] L. X. Zhu,[60] S. H. Zhu,[67] S. Q. Zhu,[40] T. J. Zhu,[74] W. J. Zhu,[11,f] Y. C. Zhu,[68,55] Z. A. Zhu,[1,60] J. H. Zou,[1] and J. Zu[68,55]

(BESIII Collaboration)

[1]*Institute of High Energy Physics, Beijing 100049, People's Republic of China*
[2]*Beihang University, Beijing 100191, People's Republic of China*
[3]*Beijing Institute of Petrochemical Technology, Beijing 102617, People's Republic of China*
[4]*Bochum Ruhr-University, D-44780 Bochum, Germany*
[5]*Carnegie Mellon University, Pittsburgh, Pennsylvania 15213, USA*
[6]*Central China Normal University, Wuhan 430079, People's Republic of China*
[7]*Central South University, Changsha 410083, People's Republic of China*
[8]*China Center of Advanced Science and Technology, Beijing 100190, People's Republic of China*
[9]*China University of Geosciences, Wuhan 430074, People's Republic of China*
[10]*COMSATS University Islamabad, Lahore Campus, Defence Road, Off Raiwind Road, 54000 Lahore, Pakistan*
[11]*Fudan University, Shanghai 200433, People's Republic of China*
[12]*G.I. Budker Institute of Nuclear Physics SB RAS (BINP), Novosibirsk 630090, Russia*
[13]*GSI Helmholtzcentre for Heavy Ion Research GmbH, D-64291 Darmstadt, Germany*
[14]*Guangxi Normal University, Guilin 541004, People's Republic of China*
[15]*Guangxi University, Nanning 530004, People's Republic of China*
[16]*Hangzhou Normal University, Hangzhou 310036, People's Republic of China*
[17]*Hebei University, Baoding 071002, People's Republic of China*
[18]*Helmholtz Institute Mainz, Staudinger Weg 18, D-55099 Mainz, Germany*
[19]*Henan Normal University, Xinxiang 453007, People's Republic of China*
[20]*Henan University of Science and Technology, Luoyang 471003, People's Republic of China*
[21]*Henan University of Technology, Zhengzhou 450001, People's Republic of China*
[22]*Huangshan College, Huangshan 245000, People's Republic of China*
[23]*Hunan Normal University, Changsha 410081, People's Republic of China*
[24]*Hunan University, Changsha 410082, People's Republic of China*
[25]*Indian Institute of Technology Madras, Chennai 600036, India*
[26]*Indiana University, Bloomington, Indiana 47405, USA*
[27a]*INFN Laboratori Nazionali di Frascati, I-00044, Frascati, Italy*
[27b]*INFN Sezione di Perugia, I-06100, Perugia, Italy*
[27c]*University of Perugia, I-06100, Perugia, Italy*
[28a]*INFN Sezione di Ferrara, I-44122, Ferrara, Italy*
[28b]*University of Ferrara, I-44122, Ferrara, Italy*
[29]*Institute of Modern Physics, Lanzhou 730000, People's Republic of China*
[30]*Institute of Physics and Technology, Peace Avenue 54B, Ulaanbaatar 13330, Mongolia*

[31]Instituto de Alta Investigacion, Universidad de Tarapaca, Casilla 7D, Arica 1000000, Chile

[32]Jilin University, Changchun 130012, People's Republic of China

[33]Johannes Gutenberg University of Mainz, Johann-Joachim-Becher-Weg 45, D-55099 Mainz, Germany

[34]Joint Institute for Nuclear Research, 141980 Dubna, Moscow Region, Russia

[35]Justus-Liebig-Universitaet Giessen, II. Physikalisches Institut, Heinrich-Buff-Ring 16, D-35392 Giessen, Germany

[36]Lanzhou University, Lanzhou 730000, People's Republic of China

[37]Liaoning Normal University, Dalian 116029, People's Republic of China

[38]Liaoning University, Shenyang 110036, People's Republic of China

[39]Nanjing Normal University, Nanjing 210023, People's Republic of China

[40]Nanjing University, Nanjing 210093, People's Republic of China

[41]Nankai University, Tianjin 300071, People's Republic of China

[42]National Centre for Nuclear Research, Warsaw 02-093, Poland

[43]North China Electric Power University, Beijing 102206, People's Republic of China

[44]Peking University, Beijing 100871, People's Republic of China

[45]Qufu Normal University, Qufu 273165, People's Republic of China

[46]Shandong Normal University, Jinan 250014, People's Republic of China

[47]Shandong University, Jinan 250100, People's Republic of China

[48]Shanghai Jiao Tong University, Shanghai 200240, People's Republic of China

[49]Shanxi Normal University, Linfen 041004, People's Republic of China

[50]Shanxi University, Taiyuan 030006, People's Republic of China

[51]Sichuan University, Chengdu 610064, People's Republic of China

[52]Soochow University, Suzhou 215006, People's Republic of China

[53]South China Normal University, Guangzhou 510006, People's Republic of China

[54]Southeast University, Nanjing 211100, People's Republic of China

[55]State Key Laboratory of Particle Detection and Electronics,
Beijing 100049, Hefei 230026, People's Republic of China

[56]Sun Yat-Sen University, Guangzhou 510275, People's Republic of China

[57]Suranaree University of Technology, University Avenue 111, Nakhon Ratchasima 30000, Thailand

[58]Tsinghua University, Beijing 100084, People's Republic of China

[59a]Turkish Accelerator Center Particle Factory Group, Istinye University, 34010, Istanbul, Turkey

[59b]Near East University, Nicosia, North Cyprus, 99138 Mersin 10, Turkey

[60]University of Chinese Academy of Sciences, Beijing 100049, People's Republic of China

[61]University of Groningen, NL-9747 AA Groningen, Netherlands

[62]University of Hawaii, Honolulu, Hawaii 96822, USA

[63]University of Jinan, Jinan 250022, People's Republic of China

[64]University of Manchester, Oxford Road, Manchester M13 9PL, United Kingdom

[65]University of Muenster, Wilhelm-Klemm-Strasse 9, 48149 Muenster, Germany

[66]University of Oxford, Keble Road, Oxford OX13RH, United Kingdom

[67]University of Science and Technology Liaoning, Anshan 114051, People's Republic of China

[68]University of Science and Technology of China, Hefei 230026, People's Republic of China

[69]University of South China, Hengyang 421001, People's Republic of China

[70]University of the Punjab, Lahore-54590, Pakistan

[71a]University of Turin and INFN, University of Turin, I-10125, Turin, Italy

[71b]University of Eastern Piedmont, I-15121, Alessandria, Italy

[71c]INFN, I-10125, Turin, Italy

[72]Uppsala University, Box 516, SE-75120 Uppsala, Sweden

[73]Wuhan University, Wuhan 430072, People's Republic of China

[74]Xinyang Normal University, Xinyang 464000, People's Republic of China

[75]Yantai University, Yantai 264005, People's Republic of China

[76]Yunnan University, Kunming 650500, People's Republic of China

[77]Zhejiang University, Hangzhou 310027, People's Republic of China

[78]Zhengzhou University, Zhengzhou 450001, People's Republic of China

Based on electron positron collision data collected with the BESIII detector operating at the BEPCII storage rings, the differential cross sections of inclusive π^0 and K_S^0 production as a function of hadron momentum, normalized by the total cross section of the $e^+e^- \to$ hadrons process, are measured at six center-of-mass energies from 2.2324 to 3.6710 GeV. Our results, which cover a relative hadron energy range from 0.1 to 0.9, significantly deviate from several theoretical calculations based on existing fragmentation functions.

Color confinement at long distance is one of the fundamental properties of quantum chromodynamics (QCD), which is the underlying theory describing the strong interactions between quarks and gluons. Because of confinement, quarks and gluons produced in hard scattering processes will ultimately become colorless hadrons. The transition from quarks q, antiquarks $\bar{q}$, and gluons g to hadrons h, which occurs at a scale with a small momentum transfer, must be treated nonperturbatively due to the large strong-coupling constant α_s [1,2]. Consequently, the fragmentation function (FF) $D_{q,\bar{q},g}^h(z,\mu_F)$ is used to describe the nonperturbative long-distance behavior associated with the hadronization process [3]. Here, μ_F is the factorization scale used to factorize the cross section in terms of the convolution of perturbative hard-part coefficients and nonperturbative fragmentation functions, and is usually set to be the center-of-mass (c.m.) energy ($\sqrt{s}$) in e^+e^- experiments. The dimensionless variable $z \equiv 2\sqrt{p_h^2 c^2 + M_h^2 c^4}/\sqrt{s}$ is the relative hadron energy, where p_h and M_h are the momentum and mass of hadron h, respectively. Single inclusive e^+e^- annihilation, $e^+e^- \to h + X$, where h is an identified hadron and X represents everything else, provides a clean way to study FFs [4]. A typical experimental observable is

$$\frac{1}{\sigma(e^+e^- \to \text{hadrons})} \frac{d\sigma(e^+e^- \to h + X)}{dp_h}, \quad (1)$$

where $\sigma(e^+e^- \to \text{hadrons})$ is the total cross section for e^+e^- annihilation to all possible hadronic final states (referred to as inclusive hadronic events hereafter). At the leading order in α_s, the observable can be interpreted as $\sum_q e_q^2 [D_q^h(z,\sqrt{s}) + D_{\bar{q}}^h(z,\sqrt{s})]$, where e_q is the fractional charge of the quark q. As summarized in Ref. [4], extensive high-precision measurements of this observable have been made in e^+e^- experiments at the c.m. energies above 10 GeV, but measurements in the region from 3.6 to 5.2 GeV have statistical uncertainties ranging from 20% to 50% [5,6].

On the other hand, remarkable progress has been made in the experimental study of nucleon structure by taking advantage of the semi-inclusive deep-inelastic scattering (SIDIS) process. Because of its explicit dependence on both the identified initial and final state hadrons, the SIDIS process plays a crucial role in probing specific quark

flavors. In particular, the FFs act as the weights used to perform flavor separation in the initial state. For example, precise kaon FFs might be the key to understanding the puzzle of the strange-quark polarization inside a longitudinally polarized proton [7,8]. The momentum-transfer Q (equivalent to $\sqrt{s}$ in e^+e^- annihilation) for the existing SIDIS data from fixed-target experiments like the ones at Jefferson Lab, COMPASS, and HERMES [9] covers the range from 1 to 10 GeV, where only sparse single inclusive e^+e^- annihilation data exist. Moreover, the proposed Electron-Ion Collider and the Electron-Ion Collider in China [10,11] would provide very high precision structure function measurements, which, in order to determine precise parton distribution functions for various quark flavors, would put unprecedented requirements on the precision of FFs for the Q value down to 1 GeV and almost complete z coverage from 0 to 1. Therefore, comprehensive investigations on the single inclusive annihilation with identified pion and kaon final states, especially in the region not well covered by previous data, will provide valuable input for the nucleon structure study.

In this Letter, the processes $e^+e^- \to \pi^0/K_S^0 + X$ are studied at six c.m. energies from 2.2324 to 3.6710 GeV, with a z coverage from 0.1 to 0.9. Data sets used in this research were collected with the BESIII detector [12] running at BEPCII. The detector has a geometrical acceptance of 93% of the 4π solid angle for the relatively stable final-state particles. It is based on a superconducting solenoid magnet with a main drift chamber as a central tracking system, plastic scintillators as a time-of-flight system, CsI crystals as an electromagnetic calorimeter (EMC) and resistive plate chambers as a muon system.

Monte Carlo (MC) simulations based on GEANT4 software [13], which includes the geometric description of the BESIII detector and implements the interactions between the final-state particles and the detector, are used to optimize the event selection criteria, estimate the number of residual background events, and determine the correction factors accounting for the efficiency loss and initial-state radiation (ISR) effects. The inclusive hadronic events are simulated with the LUARLW generator [14–16], where among others the signal processes $e^+e^- \to \pi^0/K_S^0 + X$ are contained. Background MC samples of the processes $e^+e^- \to e^+e^-$, $\mu^+\mu^-$, and $\gamma\gamma$ are generated by

TABLE I. The integrated luminosities and the total observed hadronic and residual background events at various c.m. energy points.

$\sqrt{s}$ (GeV)	$\mathcal{L}$ (pb^{-1})	$N_{\text{had}}^{\text{tot}}$	N_{bkg}
2.2324	2.645	83227	2041
2.4000	3.415	96627	2331
2.8000	3.753	83802	2075
3.0500	14.89	283822	7719
3.4000	1.733	32202	843
3.6710	4.628	75253	6461

BABAYAGA3.5 [17]. At $\sqrt{s} = 3.6710$ GeV, the $e^+e^- \rightarrow \tau^+\tau^-$ process is simulated via the KKMC [18] generator, in which the decay of τ lepton is modeled by EVTGEN [19]. The background events from the two-photon processes are simulated by the corresponding dedicated MC generators, as detailed in Ref. [16]. In addition, the beam-associated events are estimated by a sideband method.

In this analysis, the inclusive hadronic events are selected first, from which the $e^+e^- \rightarrow \pi^0/K_S^0 + X$ events are identified by reconstructing a π^0 or K_S^0 meson. We begin by removing the dominant background processes, i.e., the $e^+e^- \rightarrow e^+e^-$ and $e^+e^- \rightarrow \gamma\gamma$ events. In each remaining event, the good charged hadronic tracks are identified with the same selection criteria as described in Ref. [16], and events with at least two good tracks are kept for further analysis. For events with two or three good charged tracks, additional requirements on the charged tracks and the showers in the EMC are implemented to further suppress the background related to the quantum electrodynamics process. Events with more than three good charged tracks are retained directly without any additional requirements. The details of the selection of the inclusive hadronic events are presented in Ref. [16]. The numbers of inclusive hadronic events ($N_{\text{had}}^{\text{tot}}$) and residual background events (N_{bkg}), as well as the integrated luminosity of each data sample, are summarized in Table I.

A π^0 candidate is reconstructed via the decay $\pi^0 \rightarrow \gamma\gamma$. Photon candidates are identified using showers in the EMC. The deposited energy of each shower must be greater than 25 MeV in the barrel region ($|\cos\theta| < 0.80$) and 50 MeV in the end-cap region ($0.86 < |\cos\theta| < 0.92$), where θ is the polar angle defined with respect to the symmetry axis of the main drift chamber. The shower is required to be separated by more than 10 degrees from the closest charged track to eliminate those produced by the charged particles. The difference between the EMC time and the event start time has to be within [0, 700] ns to suppress electronic noise and showers unrelated to the event. All combinations of two photons are used to form π^0 candidates. To suppress background due to the miscombination of photons, requirements are made on the polar angle of one photon in the helicity

frame of the π^0 candidate (θ_γ). For π^0 candidates with momentum less than 0.3 GeV/c, $|\cos\theta_\gamma|$ is required to be less than 0.8, while for those with momentum larger than 0.3 GeV/c, it must be less than 0.95. Each π^0 candidate in an event is counted as a candidate of the separate inclusive π^0 event, and the fraction of the observed hadronic events containing more than one π^0 meson varies from 42% to 50% at the c.m. energies from $\sqrt{s} = 2.2324$ to 3.6710 GeV.

A K_S^0 candidate is formed by combining a pair of oppositely charged tracks. The two tracks are required to satisfy $|\cos\theta| < 0.93$. Because of the relatively long lifetime of the K_S^0 meson, the distance of closest approach of these charged tracks from the interaction point must be less than 30 cm along and 10 cm perpendicular to the beam direction. As a result of the different requirements, the charged track here is not necessarily one of the good charged tracks identified previously. To increase the number of events, no particle identification is applied. Furthermore, to select K_S^0 signal events, the production and decay vertices of K_S^0 are reconstructed, and the decay length between these two vertices is required to be at least twice its uncertainty. Each K_S^0 candidate in an event is counted as a candidate of the separate inclusive K_S^0 event. In this measurement, fewer than 1% observed hadronic events contain more than one K_S^0 meson.

After imposing the above selection criteria, the residual contributions to the mass spectra of the photon and charged-pion pairs, $M(\gamma\gamma)$ and $M(\pi^+\pi^-)$, from lepton-pair production, two-photon processes, and beam-associated events are less than 0.1% in both signal processes. The dominant background is caused by the miscombinations of the corresponding daughter particles, which are reproduced by the inclusive hadronic MC samples and well described by a polynomial.

The $M(\gamma\gamma)$ and $M(\pi^+\pi^-)$ spectra are divided into the momentum intervals with a step of $\Delta p_{\pi^0/K_S^0} = 0.1$ GeV/c, which is 5 times larger than the corresponding momentum resolutions. Unbinned maximum likelihood fits are performed on the $M(\gamma\gamma)$ and $M(\pi^+\pi^-)$ spectra obtained in each momentum interval to determine the corresponding numbers of signal events, i.e., $N_{\pi^0}^{\text{obs}}$ and $N_{K_S^0}^{\text{obs}}$. For the $e^+e^- \rightarrow \pi^0 + X$ candidates, the signal is described by a Crystal Ball function [20], while the background is parametrized by a second-order Chebyshev polynomial. For the $e^+e^- \rightarrow K_S^0 + X$ process, the signal is modeled by a double Gaussian function, and the background is described by a first-order Chebyshev polynomial. Figure 1 illustrates the fit results of the π^0 and K_S^0 candidates with $p_{\gamma\gamma/\pi^+\pi^-} \in (0.4, 0.5)$ GeV/c in the data sample at $\sqrt{s} = 2.8000$ GeV. The summary of $N_{\pi^0}^{\text{obs}}$ and $N_{K_S^0}^{\text{obs}}$ obtained in each momentum range at each c.m. energy is given in Supplemental Material [21].
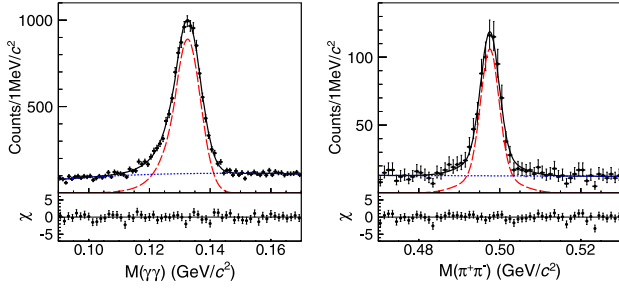
FIG. 1. The $M(\gamma\gamma)$ and $M(\pi\pi)$ distributions for π^0 (left) and K_S^0 (right) candidates with $p_{\gamma\gamma/\pi^+\pi^-} \in (0.4, 0.5)$ GeV/c at $\sqrt{s} = 2.8000$ GeV. The fit results are overlaid. The black points with error bars are data. The black solid curves are the sum of fit functions, while the red dashed and blue dotted curves represent the signal and background, respectively. The pull variable χ, defined as the residual between the data and the total fit function, normalized by the uncertainty of the data, is shown on the bottom of the figures.

In practice, the normalized differential cross section for the inclusive production of any identified hadron, namely Eq. (1), is determined with

$$\frac{N_h^{\text{obs}}}{N_{\text{had}}^{\text{obs}}} \frac{1}{\Delta p_h} f_h, \quad (2)$$

where $N_{\text{had}}^{\text{obs}} = N_{\text{had}}^{\text{tot}} - N_{\text{bkg}}$ is the net number of observed hadronic events in e^+e^- annihilation at a given c.m. energy, N_h^{obs} is that of the $e^+e^- \to h + X$ events within a specific momentum range Δp_h, and f_h is a correction factor which accounts for the effects caused by the limited detector acceptance, the selection criteria, ISR, and vacuum polarization. Since both $N_{\text{had}}^{\text{obs}}$ and N_h^{obs} are obtained from the same data sample, the integrated luminosity usually used in the cross section measurement cancels.

In this analysis, the correction factor f_h is obtained from the signal MC sample and is given by

$$f_h = \frac{\bar{N}_h^{\text{tru}}(\text{off})}{\bar{N}_{\text{had}}^{\text{tru}}(\text{off})} \Big/ \frac{\bar{N}_h^{\text{obs}}(\text{on})}{\bar{N}_{\text{had}}^{\text{obs}}(\text{on})}, \quad (3)$$

where the variable "$\bar{N}$" denotes the numbers of events determined from the signal MC sample, either at the detector observed level, similar to the experimental data, with superscript "obs" or at the generation level with superscript "tru." The terms "on" and "off" in the parentheses indicate that the corresponding quantities are obtained from signal MC samples with and without simulating the ISR effects, respectively. $\bar{N}_h^{\text{obs}}(\text{on})$ is determined by applying the same fit procedure on the signal MC events as data. By definition, f_h compensates the event lost caused by the limited acceptance of the BESIII detector in the small polar angle region [21]. In this analysis, the correction factor f_h is by far dominated by the detection efficiency. Calculated results of f_h in different momentum ranges for π^0 and K_S^0 are presented in Supplemental Material [21].

The systematic uncertainties of the normalized differential cross section measurements mainly originate from the differences between the signal MC and data samples, the reconstruction efficiencies of the π^0 and K_S^0 candidates, the fits to the $M(\gamma\gamma)$ and $M(\pi^+\pi^-)$ spectra, and the MC simulation model of the inclusive hadronic events. To estimate the uncertainty caused by the imperfect simulation of various kinematic variables of the signal events, all the selection criteria are separately varied to be larger or smaller than their nominal values by one time their resolutions, and the maximum changes of the normalized differential cross sections are taken as the systematic uncertainties. The uncertainty in the photon detection efficiency is estimated to be 1% per photon [22], therefore 2% is taken as the systematic uncertainty due to the π^0 reconstruction efficiency where the complete correlation between the detection of the two photons is assumed. The momentum-dependent systematic uncertainties due to the K_S^0 reconstruction efficiency are obtained by applying a dedicated weighting procedure [23], which incorporates weights due to the charged particle tracking efficiency and the decay length requirement.

The uncertainties due to the fits on the $M(\gamma\gamma)$ and $M(\pi^+\pi^-)$ distributions are examined by using alternative signal and background shapes. The alternative signal shape of $e^+e^- \to \pi^0 + X$ is taken as the shape from the signal MC sample, while that for $e^+e^- \to K_S^0 + X$ is chosen as a single Gaussian function. The alternative background shapes are obtained by varying the order of the Chebyshev polynomials. The relative differences from the nominal differential cross sections are taken as the corresponding systematic uncertainties.

The dominant source of systematic uncertainty is the MC simulation model of the inclusive hadronic events. The generation fractions of the exclusive processes containing π^0 and K_S^0, which make up the inclusive process, directly affect the correction factors f_{π^0} and $f_{K_S^0}$. To address the corresponding uncertainty, the HYBRID generator, which was developed in Ref. [24] and improved in Ref. [16], is used as an alternative MC model to generate the inclusive hadronic events. In the HYBRID generator, much knowledge of the allowed exclusive processes in the c.m. energy region of BESIII has been incorporated, including measured cross sections and production mechanisms. In addition, a different simulation scheme of the ISR process is adopted [16]. The changes of the correction factors f_{π^0} and $f_{K_S^0}$ are assigned as the systematic uncertainties. All these individual systematic uncertainties are regarded as uncorrelated with each other and are summed in quadrature.

The normalized differential cross sections for the inclusive π^0 and K_S^0 production in e^+e^- annihilation at the six c.m. energies are tabulated in Supplemental Material [21] and shown in Figs. 2 and 3, respectively. Figure 2 also shows various theoretical predictions extrapolated from
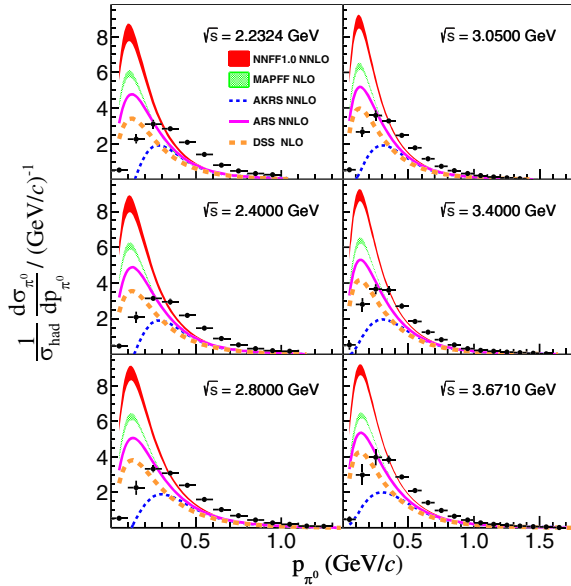
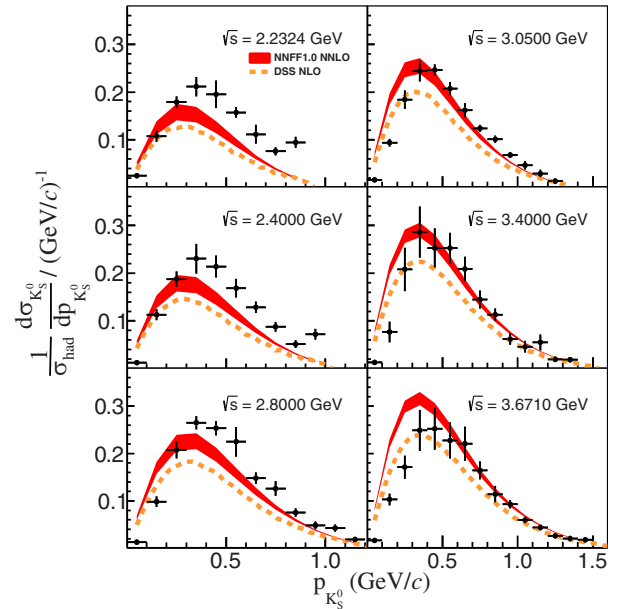FIG. 2. Normalized differential cross sections of the $e^+e^- \to \pi^0 + X$ process. The points with error bars are the measured values, where the uncertainties are the quadrature sum of the corresponding statistical and systematic uncertainties. The bands or curves in red, green, blue, magenta, and orange denote the NNFF, MAPFF, AKRS, ARS, and DSS calculations, respectively, where only the former two cover $\pm 1\sigma$ limits. Normalized differential cross sections as function of z are shown in Supplemental Material [21].

FIG. 3. Normalized differential cross sections of the $e^+e^- \to K_S^0 + X$ process. The points with error bars are the measured values, where the uncertainties are the quadrature sum of the corresponding statistical and systematic uncertainties. The red band shows the theoretical calculation from NNFF with $\pm 1\sigma$ limits and the orange curve denotes the prediction of DDS. Normalized differential cross sections as function of z are shown in Supplemental Material [21].

different FFs determined from existing world data [4]. The FFs are obtained with slightly different assumptions and show the sensitivity of the prediction to assumptions about the behavior at low-z and different $\sqrt{s}$. ARS [25], AKRS [26], and NNFF1.0 [27] are all obtained from inclusive annihilation data at NNLO accuracy. However, AKRS includes small-z resummation, NNFF1.0 includes hadron-mass corrections and all of them have different initial evolution scales and kinematics requirements on the data. The MAPFF1.0 NLO study [28] contains low-Q^2 data from the lepton-proton fixed-target experiments at HERMES [29] and COMPASS [30]. The DSS NLO calculation [31] contains low-Q^2 data from the lepton-proton fixed-target experiments at HERMES and single inclusive production of proton-proton collisions. Figure 3 shows the comparison of the normalized differential cross section of the inclusive K_S^0 production with predictions from NNFF1.0 at NNLO precision and DSS at NLO precision. In these comparisons, the disagreement is observed to depend on both c.m. energy and hadron momentum. Here, the FFs are further away from the kinematic region of the original data. One possible reason for these discrepancies is that a calculation restricted to the leading twist may not be sufficient at the BESIII energy scale. It may also be important to consider quark mass and hadron mass correction effects [32], and small-z resummation effects [26]. Another problem may be

associated with the extrapolation of the FFs from existing e^+e^- annihilation data at high energy to the low-energy scale at BESIII. For instance, the predictions using QCD-backward evolution for initial-state parton distribution functions from high to low energies have been found to deviate from the experimental measurements [33]. Both Figs. 2 and 3 show that BESIII data can be used to improve the fit procedure to determine the FFs at the low energy scale. Also, the difference between primary and secondary processes has to be taken into account as well. Studies based on the signal MC samples show that the $\rho^\pm$ (K^*) decay has contribution to the inclusive π^0 (K_S^0) production in the c.m. energy region of this analysis. The results presented in this Letter will be key to explore these possibilities as well as help to test collinear perturbative QCD with data at the relatively low energy scale.

In summary, we have measured the normalized differential cross sections of the $e^+e^- \to \pi^0/K_S^0 + X$ processes, using data samples collected from $\sqrt{s} = 2.2324$ to 3.6710 GeV. The results obtained in this work help to fill the region with $\sqrt{s} < 10$ GeV where precision e^+e^- annihilation data have been rarely reported. The results provide broad z coverage from 0.1 to 0.9 with precision of around 3% at $z \sim 0.4$. These results provide new ingredients for FF global data fits, in which almost no single inclusive annihilation data measured in this special energy region has been included.

---

[a] Also at the Moscow Institute of Physics and Technology, Moscow 141700, Russia.

[b] Also at the Novosibirsk State University, Novosibirsk, 630090, Russia.

[c] Also at the NRC "Kurchatov Institute," PNPI, 188300, Gatchina, Russia.

[d] Also at Goethe University Frankfurt, 60323 Frankfurt am Main, Germany.

[e] Also at Key Laboratory for Particle Physics, Astrophysics and Cosmology, Ministry of Education; Shanghai Key Laboratory for Particle Physics and Cosmology; Institute of Nuclear and Particle Physics, Shanghai 200240, People's Republic of China.

[f] Also at Key Laboratory of Nuclear Physics and Ion-beam Application (MOE) and Institute of Modern Physics, Fudan University, Shanghai 200443, People's Republic of China.

[g] Also at State Key Laboratory of Nuclear Physics and Technology, Peking University, Beijing 100871, People's Republic of China.

[h] Also at School of Physics and Electronics, Hunan University, Changsha 410082, China.

[i] Also at Guangdong Provincial Key Laboratory of Nuclear Science, Institute of Quantum Matter, South China Normal University, Guangzhou 510006, China.

[j] Also at Frontiers Science Center for Rare Isotopes, Lanzhou University, Lanzhou 730000, People's Republic of China.

[k] Also at Lanzhou Center for Theoretical Physics, Lanzhou University, Lanzhou 730000, People's Republic of China.

[l] Also at the Department of Mathematical Sciences, IBA, Karachi, Pakistan.

[m] Now at Zhejiang Jiaxing Digital City Laboratory Co., Ltd, Jiaxing 314051, People's Republic of China.

[1] M. Schmelling, Phys. Scr. **51**, 683 (1995).

[2] D. d'Enterria *et al.*, arXiv:2203.08271.

[3] A. Metz and A. Vossen, Prog. Part. Nucl. Phys. **91**, 136 (2016).

[4] P. A. Zyla *et al.* (Particle Data Group), Prog. Theor. Exp. Phys. **2020**, 083C01 (2020).

[5] R. Brandelik *et al.* (DASP Collaboration), Nucl. Phys. **B148**, 189 (1979).

[6] J. Burmester *et al.* (PLUTO Collaboration), Phys. Lett. **67B**, 367 (1977).

[7] E. Leader, A. V. Sidorov, and D. B. Stamenov, Phys. Rev. D **84**, 014002 (2011).

[8] E. Leader, A. V. Sidorov, and D. B. Stamenov, Phys. Rev. D **91**, 054017 (2015).

[9] A. Deur, S. J. Brodsky, and G. F. De Téramond, Rep. Prog. Phys. **82**, 076201 (2019).

[10] A. Accardi *et al.*, Eur. Phys. J. A **52**, 268 (2016).

[11] D. P. Anderle *et al.*, Front. Phys. (Beijing) **16**, 64701 (2021).

[12] M. Ablikim *et al.* (BESIII Collaboration), Nucl. Instrum. Methods Phys. Res., Sect. A **614**, 345 (2010).

[13] S. Agostinelli *et al.* (GEANT4 Collaboration), Nucl. Instrum. Methods Phys. Res., Sect. A **506**, 250 (2003).

[14] B. Andersson, *The Lund Model* (Cambridge University Press, Cambridge, England, 1998).

[15] B. Andersson and H. M. Hu, arXiv:9910285.

[16] M. Ablikim *et al.* (BESIII Collaboration), Phys. Rev. Lett. **128**, 062004 (2022).

[17] C. M. Carloni Calame, C. Lunardini, G. Montagna, O. Nicrosini, and F. Piccinini, Nucl. Phys. **B584**, 459 (2000).

[18] S. Jadach, B. F. L. Ward, and Z. Was, Comput. Phys. Commun. **130**, 260 (2000).

[19] D. J. Lange, Nucl. Instrum. Methods Phys. Res., Sect. A **462**, 152 (2001).

[20] T. Skwarnicki, Ph.D. thesis, Institute of Nuclear Physics, Krakow, Report No. DESY-F31-86-02, 1986.

[21] See Supplemental Material at http://link.aps.org/supplemental/10.1103/PhysRevLett.130.231901 for more details of this analysis.

[22] M. Ablikim *et al.* (BESIII Collaboration), Phys. Rev. D **99,** 011101 (2019).

[23] M. Ablikim *et al.* (BESIII Collaboration), Phys. Rev. D **92,** 112008 (2015).

[24] R. G. Ping *et al.*, Chin. Phys. C **40,** 113002 (2016).

[25] D. P. Anderle, M. Stratmann, and F. Ringer, Phys. Rev. D **92,** 114017 (2015).

[26] D. P. Anderle, T. Kaufmann, M. Stratmann, and F. Ringer, Phys. Rev. D **95,** 054003 (2017).

[27] V. Bertone, S. Carrazza, N. P. Hartland, E. R. Nocera, and J. Rojo (NNPDF Collaboration), Eur. Phys. J. C **77,** 516 (2017).

[28] R. Abdul Khalek, V. Bertone, and E. R. Nocera, Phys. Rev. D **104,** 034007 (2021).

[29] A. Airapetian *et al.* (HERMES Collaboration), Phys. Rev. D **87,** 074029 (2013).

[30] C. Adolph *et al.* (COMPASS Collaboration), Phys. Lett. B **764,** 1 (2017).

[31] D. de Florian, R. Sassot, and M. Stratmann, Phys. Rev. D **75,** 114010 (2007).

[32] A. Accardi, D. P. Anderle, and F. Ringer, Phys. Rev. D **91,** 034008 (2015).

[33] F. Caola, S. Forte, and J. Rojo, Nucl. Phys. **A854,** 32 (2011).